IMPROVEMENT OF WOOD CT IMAGES BY CONSIDERATION OF THE SKEWING OF ULTRASOUND CAUSED BY GROWTH RING ANGLE

Kwang-Mo Kim[1]
Research Scientist
Department of Forest Products
Korea Forest Research Institute
Seoul, 130-712, Korea

Jun-Jae Lee[1]
Professor

Sang-Joon Lee
Graduate Research Assistant

*Hwanmyeong Yeo**†
Assistant Professor
Department of Forest Sciences
Research Institute for Agriculture and Life Science
Seoul National University
Seoul, 151-921, Korea

(Received January 2008)

Abstract. For the purpose of removing distortions in ultrasonic computerized tomographic (CT) images of wood, this study proposes a technique for taking into account the skewing effect in reconstructing the image. First, it was experimentally confirmed that an ultrasonic wave is refracted because of the anisotropic characteristics of wood. Transmission paths of an ultrasonic wave through a cross-section of wood were predicted by considering the change in wave velocity based on the annual ring angle and the presence of juvenile wood. Then, the methodology of the application of the predicted paths to CT image reconstruction was proposed and verified. The accuracy of defect detection in wood was significantly improved by the proposed technique.

Keywords: Ultrasonic wave, computed tomography (CT), transmission path, skewing effect, wave refraction, juvenile wood.

INTRODUCTION

This study was carried out as part of a research project aimed at developing an ultrasonic computed tomographic (CT) system for wood in field applications. In a previous part of the project, a new ultrasonic transducer was developed to compensate for the high damping characteristic of wood, and modified equipment setups and measuring procedures were proposed for field applications of the CT technology (Tamura et al 1997; Adachi et al 1999). In addition, well-known existing algorithms, such as the filtered back-projection method and the simultaneous iterative reconstruction technique, were modified to reconstruct CT images from incomplete time-of-flight profiles (Kim and Lee 2005a, b; Yanagida et al 2007).

However, there were some image distortions in the CT images obtained. The detected defects were enlarged, and their shapes were found to be

[1] Joint first authors.
* Corresponding author: hyeo@snu.ac.kr
† SWST member.

distorted. The positions of the defects, in particular, were somewhat shifted to the surface of the specimen in the CT image. To find the reasons for the image distortion, Kim et al (2007) investigated the variation of wave velocities on the cross-section of a life-sized wooden structural member. From the results of the study, they concluded that the ultrasound was heavily influenced by the skewing effect in wood.

The skewing effect causes ultrasonic waves to be aligned with the stiffer direction in anisotropic material (Biernacki and Beall 1993; Dickens et al 1996; Han et al 2005). This has also been asserted by several research groups that have tried to apply the ultrasonic CT technique to wood. However, in their studies, the skewing effect was not considered in the reconstruction of CT images (Yomikawa et al 1986; Adachi et al 1994; Kanda et al 1998).

This study aims to propose a technique for incorporating the skewing effect in the reconstruction of a CT image of wood. First, we try to ascertain the transmission path of an ultrasonic wave in a cross-section of wood. For this purpose, ultrasonic wavepaths were estimated by considering the skewing effect, and the sound velocities of these paths were predicted. Then, by comparing the predicted sound velocities with the actual values, the wavepaths were adjusted. To test the technique, some ultrasonic CT images were reconstructed by using the estimated wavepaths.

MATERIALS AND METHODS

All of the data used in this paper were from our previous study (Kim et al 2007); therefore, only a brief explanation regarding testing materials and methods is presented.

Materials and Measurement

Five black locust (*Robinia pseudoacacia* L.) disks were used as specimens. The size of the specimens was 200-mm dia and 30-mm thick. The ultrasonic velocities of all specimens were measured at eight measuring angles, at 20° intervals from 40° to 180°. The measuring angle is the angle between two lines from the center of the specimen to the source and the receiver. Then, a specimen was selected to make an artificially defective specimen. The diameter of a hole-type defect was increased from 6 to 40 mm in seven steps. For each step, the same measuring process was repeated.

Estimation of Wavepaths

Kim et al (2007) measured the sound velocities of small clear black locust specimens (30 × 30 × 30 mm) which had a relatively constant annual ring angle, other than for juvenile wood. Then, they derived Eq 1, the predictor of sound velocity v_θ as a function of the annual ring angle θ.

$$\upsilon_\theta = \frac{2.0 \times 1.3}{2.0 \times \sin^{1.8}\theta + 1.3 \times \cos^{1.8}\theta} \quad (1)$$

The ultrasound transmission path for each measuring angle was traced by applying the basic concept of a brute-force approach method, proposed by Schneider et al (1992). It was assumed that the pith was positioned in the exact center of the specimen, and the annual rings were perfect circles.

As shown in Fig 1, the line connecting the source and the receiver was divided into 20 sections of the same length, and a cross-line (L_a, L_b, L_c . . .) was drawn at each node. An ultrasonic wave triggered at the source will arrive at every point on the line L_a with different travel times. We found the point of the shortest travel time using another assumption that ultrasound goes straight between the source and line L_a. The distance and annual ring angle were easily calculated from the coordinates of the source and a point on the line, and the wave velocity was obtained by using Eq 1. The travel time for every point on line L_a was calculated from the distance and velocity, and the point of the shortest travel time was selected between the points a′ and a″ as ⓐ in Fig 1.

After substituting point ⓐ for the source, the point for the shortest travel time on line L_b was determined by the same process. This process

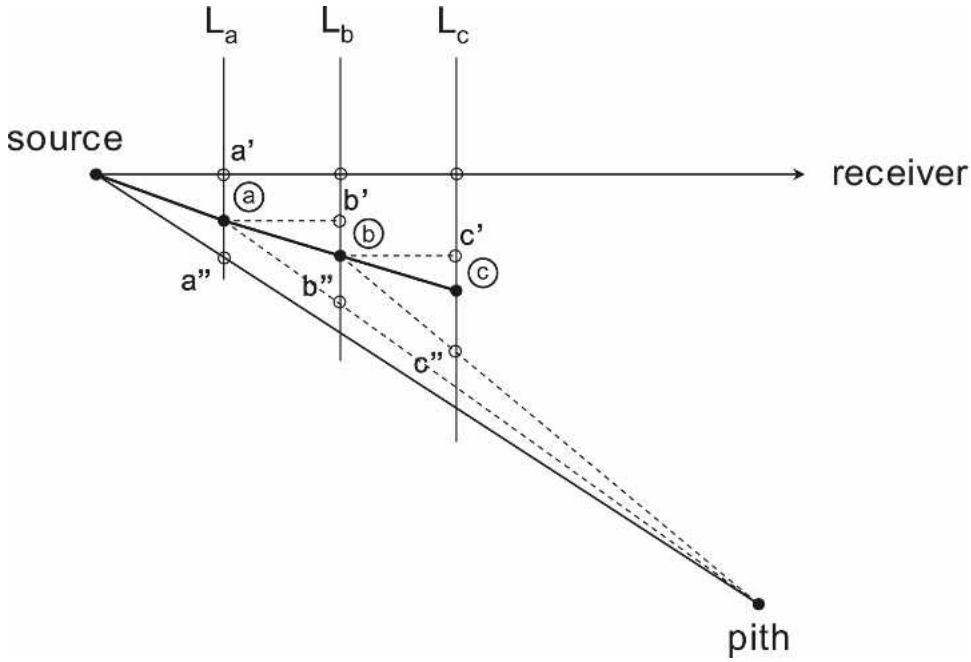

Figure 1. Estimation process for refracted wavepath using sound velocity as a function of annual ring angle.

was repeated 10 times until the wave reached the center line between the source and the receiver. Then the remaining path was considered to be symmetrical to the center line. By summing up the shortest travel times of all the sections, the ultrasonic time-of-flight (TOF) was obtained. The wave velocity of each measuring angle was calculated by dividing the straight distance between the source and the receiver by the TOF.

Reconstruction of CT Images

CT images of an artificially defective disk of wood were reconstructed by applying the wavepaths as illustrated in Figs 1, 2, and 3. Between the 9th and 10th stage of the image reconstruction process proposed by Kim et al (2007), the wavepaths were used to determine which pixel existed on the wavepath of each measurement (Fig 2).

RESULTS AND DISCUSSION

Transmission Path of Ultrasonic Wave on Wood Cross-section

The straight paths between the source and the receiver are shown in Fig 3a, and an ultrasonic wave should move along these paths in isotropic material. The refracted wavepaths estimated by considering the anisotropic characteristic of wood are also shown in Fig 3b. Because the ultrasonic velocity was greater in the direction of the smaller annual ring angle, almost all of the wavepaths were predicted to be somewhat bent toward the center of the specimen, but the level of refraction was estimated to be different for each measuring angle.

Ultrasonic Velocities Dependence on Measuring Angles

The wave velocities calculated for each refracted path are shown in Fig 4. In the figure, the calculated velocities of straight paths and the measured results are shown together (Kim et al 2007). The wave velocities of refracted paths were greater than those of straight paths by about 7%. As the level of refraction increased in Fig 3b, the velocity difference between the straight and the refracted paths also increased. The difference was at its maximum (about 17%) at the 140° measuring angle.

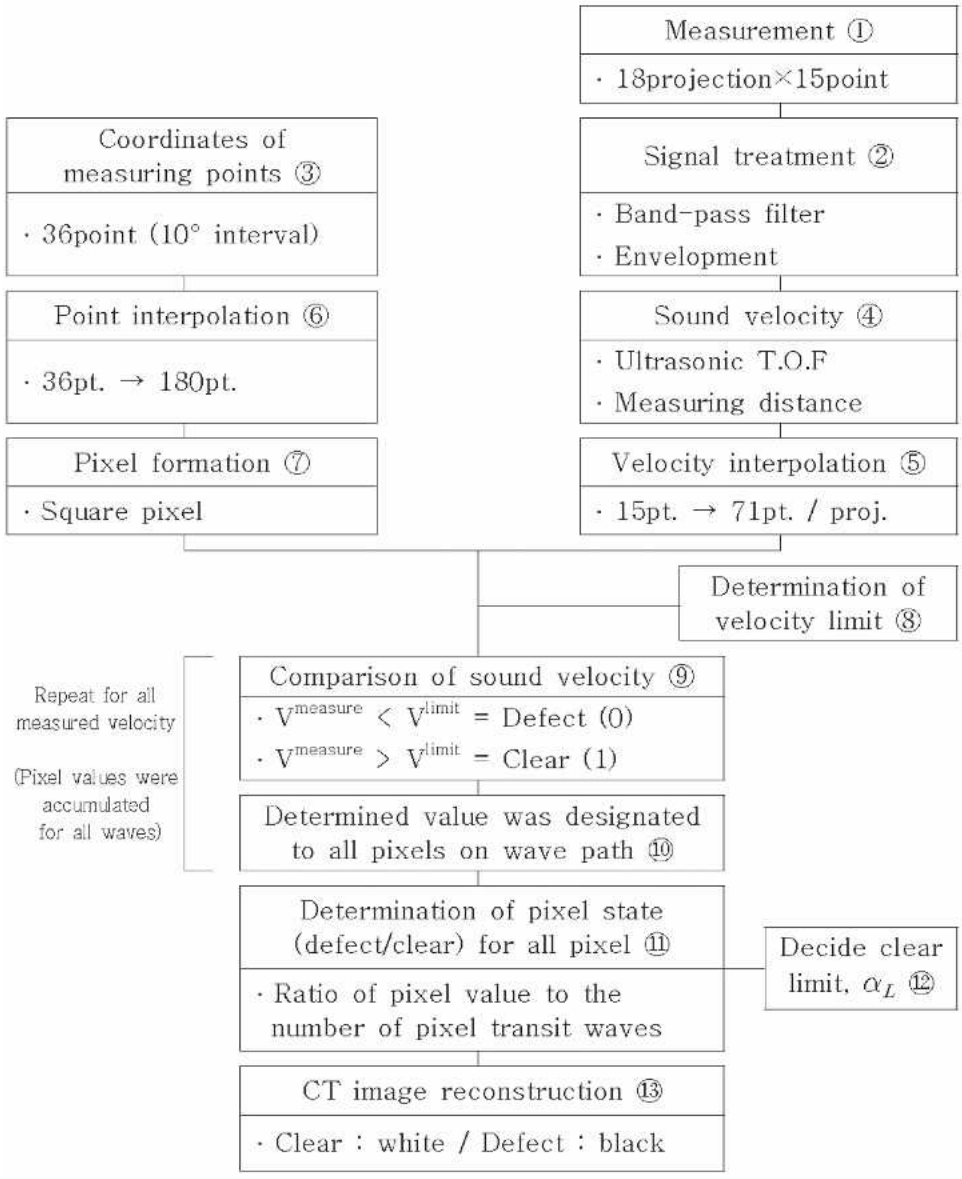

Figure 2. Flowchart for reconstruction of a cross-sectional image (Kim et al 2007).

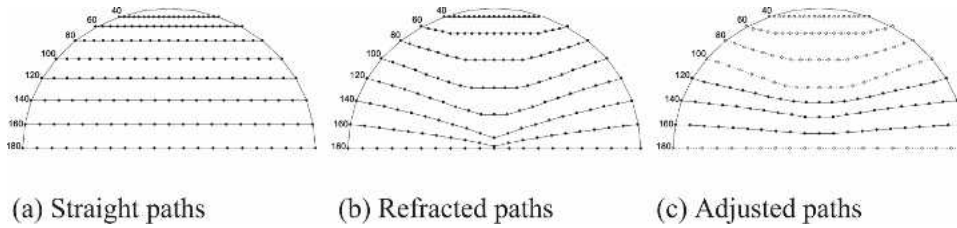

(a) Straight paths (b) Refracted paths (c) Adjusted paths

Figure 3. Transmission paths of an ultrasonic wave through a wood cross-section.

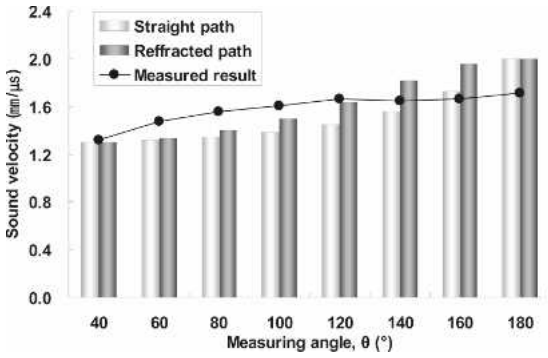

Figure 4. Measured and calculated sound velocity for each measuring angle.

When the predicted velocities were compared with the measured results, the predicted velocities were lower by about 5–10% at measuring angles of 60, 80, and 100°. This was thought to be caused by an error in the measuring position. The position of the source and the receiver was assumed to be a point in the estimating process of the wavepath, but the transducer made contact with the specimen with a circular face of 10-mm dia in the measuring process. As a result, some errors may be included in the travel distance of the ultrasonic wave. This error would increase as the measuring angle decreases.

In addition, as the measuring angle decreases, the influence of the surface wave would increase. Because a surface wave is slower than a longitudinal or transverse wave, it generally does not influence the ultrasonic measurement. But if the measuring angle is too small, a surface wave will arrive at the receiver just after the main signal with high energy intensity. Also, the surface wave makes it difficult to determine the arrival time of the main signal. The effect of the surface wave was thought to be the reason for decrease in error at 40 and 60°.

The predicted velocities were faster than the measured results at 140, 160, and 180°. This difference was thought to be caused by the presence of juvenile wood at the center of the specimen. As the measuring angle increased, the effect of juvenile wood on wave velocity also increased.

Adjustment of Wavepath by Considering Juvenile Wood

Because the sound velocity in juvenile wood is slower than that of sound wood (Han et al 2005), the level of refraction was expected to decrease. To compensate for the error caused by the presence of juvenile wood, the positional range and the sound velocity variation of juvenile wood should be determined in advance; however, it is difficult to measure these properties with a method that is nondestructive.

In this study, a simple and intuitive method for modifying the predicted wavepaths was proposed by considering the presence of juvenile wood. The wavepaths at the measuring angles of 120, 140, and 160° were determined as below to make the spaces between adjacent paths comparatively constant.

In the case of the 140 and 160° measuring angles, the wavepath in Fig 3b showed an abrupt refraction at the center point. But this kind of abrupt refraction was thought unreasonable in continuum material without an internal boundary. Therefore, the central part of the refracted path was changed to be horizontal. Then the adjusted paths in Fig 3c were determined to be at the center of the straight and refracted path of each measuring angle.

When the path at 120° was adjusted in the same manner, the adjusted path at 120° overlapped with the path at 100° in the central part. Because the effect of juvenile wood on the wavepath at 120° was expected to be smaller than that at 140 and 160°, the adjusted path for 120° was simply located at the center of the 100 and 140° wavepaths.

The ultrasonic wave velocities calculated for the adjusted wavepaths are shown in Fig 5. Because the wavepaths at measuring angles of up to 100° were not influenced by juvenile wood, the positional range of the juvenile wood was assumed to be 40% of the radius of the specimen. Also, the sound velocity of juvenile wood was assumed to be 90% of that of the sound wood.

The difference between the measured and the

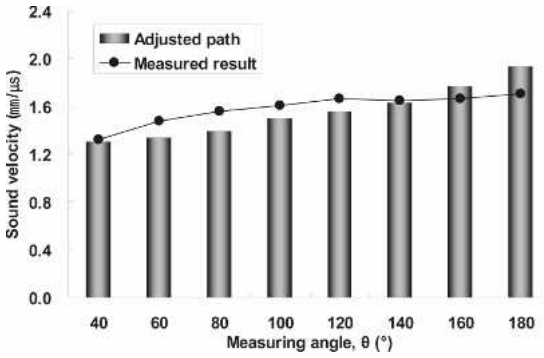

Figure 5. Sound velocities calculated for adjusted paths.

calculated velocities was reduced when the effect of juvenile wood was considered; however, it was still large at 180°, the wavepath of which did not change at any stage of this study. This was thought to be caused by the overestimation of the sound velocity of juvenile wood. When the sound velocity of juvenile wood was assumed to be 70% of that of mature wood, the calculated velocities more closely approached the measured results. However, it was difficult to draw any conclusions on the sound velocity of juvenile wood only from the results of this study.

CT Image Reconstruction of Artificially Defective Specimens

In Fig 6, CT images reconstructed by applying the three kinds of wavepaths in Fig 3 are shown. When the straight paths were applied, the sizes of detected defects were enlarged and their positions somewhat shifted to the surface of specimens on the images (Fig 6a). The CT image was reconstructed based on the assumption that an ultrasonic wave was transferred along the dashed lines of Fig 7. However, an ultrasonic wave was transferred along the solid lines due to the skewing effect. In the case of Receiver 1, although there was a defect on the straight path, the travel time was not delayed because the arriving signal passed around the defect. On the other hand, the travel time of the signal received at Receiver 2 was delayed. For these reasons, the position of the defect on the CT image was shifted to the surface of the specimen.

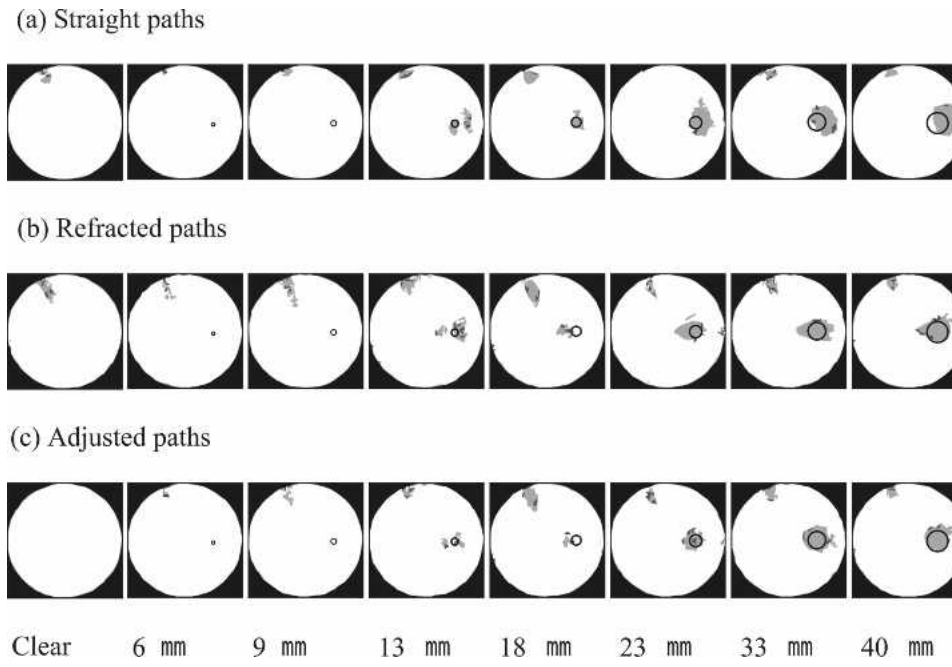

Figure 6. Reconstructed CT images of a wood disk for each defect size.

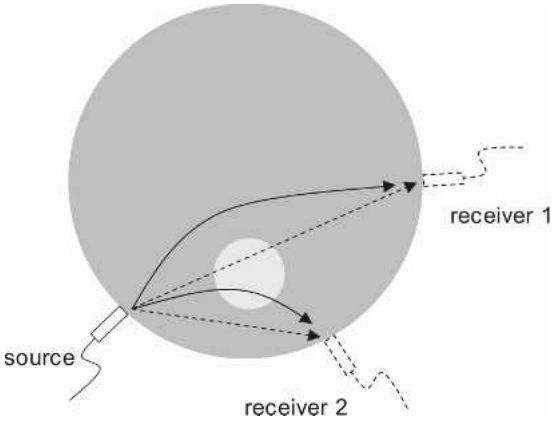

Figure 7. Image distortion caused by the skewing effect in a wood disk.

The CT images in Fig 6b were reconstructed by taking into account the wave refraction in wood, and it was confirmed that the detection accuracy of the defect position was improved remarkably. There was a tight knot at the upper left quadrant of the specimen, and its shape was thin and long. The knot was detected on almost all of the CT images, but the shape was more similar to the actual condition when the wave refraction was considered.

However, the shapes of the detected defects were slightly expanded to the center of the specimen. This was thought to occur because of the overestimation of wave refraction for the larger measuring angles because the effect of juvenile wood was not considered.

For the CT images of Fig 6c reconstructed by applying the adjusted paths, artificial defects over 23-mm dia were detected very accurately. The artificial defects of 13 and 18-mm dia were detected on the CT images, but the positions and shapes were somewhat different from the actual conditions. The reason was thought to be that the effect of the measuring error was exaggerated because the diameter of the artificial defect was smaller than the wavelength of the ultrasonic wave (about 22 mm).

From the above results, the adjusted paths in Fig 3c could be verified to precisely show the ultrasonic wavepath in wood. But this study was performed for only one species and on a small portion of a specimen. Therefore it is not reasonable to directly apply the wavepaths estimated in this study to improvement of any other ultrasonic CT system. This study was aimed only at proposing a methodology for predicting the wavepaths in wood by considering the skewing effect and applying the predicted wavepaths to the process for CT image reconstruction.

CONCLUSIONS

It was experimentally confirmed that an ultrasonic wave was refracted in wood by the anisotropy of the wood structure. Wavepaths were predicted at different measuring angles by considering the variations in wave velocity caused by the changes in the annual ring angle and the presence of juvenile wood. The methodology of the application of the predicted paths to the process of CT image reconstruction was proposed and verified. By using this technique, the accuracy of defect detection in wood can be significantly improved.

REFERENCES

Adachi K, Tamura Y, Hayashi K (1994) Cross-sectional imaging of wooden pillars with ultrasonic time-of-flight CT. Pp 279–284 *in* Proc. 29th International Symposium on Archaeometry. Ankara, Turkey.

———, ———, Kanda S, Shioya K, Yamashita Y (1999) Development of ultrasonic time-of-flight computed tomography system for structural inspection of buildings. Technical Report of IEICE, US99-9. The Institute of Electronics Information and Communication Engineers. Pp 7–14.

Biernacki JM, Beall FC (1993) Development of an acoustic-ultrasonic scanning system for nondestructive evaluation of wood and wood laminates. Wood Fiber Sci 25(3):289–297.

Dickens JR, Bender DA, Bray DE (1996) A critical-angle ultrasonic technique for the inspection of wood parallel-to-grain. Wood Fiber Sci 28(3):380–388.

Han SR, Park CY, Lee IC, Lee JJ (2005) Studies about the effect factors on ultrasonic velocity of domestic red pine. Pp 149–150 *in* Proc of International Symposium on Wood Science and Technology.

Kanda S, Shioya K, Yanagiya Y, Tamura Y, Adachi K (1998) Ultrasonic TOF-CT system for wooden pillars. Pp 743–746 *in* IEEE Ultrasonics Symposium.

Kim KM, Lee JJ (2005a) CT image reconstruction of wood by using ultrasound velocities. I. Effects of reconstruction algorithms and wood characteristics. J Korean Wood Sci Technol 33(5):21–28.

———, ——— (2005b) CT image reconstruction of wood by using ultrasound velocities. II. Determination of the initial model function of the SIRT method. J Korean Wood Sci Technol 33(5):29–37.

———, Lee SJ, Lee JJ (2007) Cross-sectional image reconstruction of wooden member by considering variation of wave velocities. J Korean Wood Sci Technol 35(5):16–23.

Schneider WA Jr., Ranzinger KA, Balch AH, Kruse C (1992) A dynamic programming approach to first arrival travel-time computation in media with arbitrarily distributed velocities. Geophysics 57(1):39–50.

Tamura Y, Adachi K, Yanagiya Y, Makino M, Shioya K (1997) Ultrasonic time-of-flight computed tomography for investigation of wooden pillars: Image reconstruction from incomplete time-of-flight profiles. Jpn J Appl Phys 36(5B):3278–3280.

Yanagida H, Tamura Y, Kim KM, Lee JJ (2007) Development of ultrasonic time-of-flight computed tomography for hardwood with anisotropic acoustic property. Jpn J Appl Phys 46(8A):5321–5325.

Yomikawa Y, Iwase Y, Arita K, Yamada H (1986) Nondestructive inspection of a wooden pole using ultrasonic computed tomography. IEEE Trans Ultrason Ferroelectr Freq Control UFFC-33(4):354–357.